Heavy hydrogen isotopes ^{4}H and ^{5}H.

L.V.Chulkov for S135 collaboration [a,1]

[a] *Gesellschaft für Schwerionenforschung (GSI), D–64291 Darmstadt, Germany*

Abstract

The hydrogen isotopes ^{4}H and ^{5}H have been investigated in the one-proton knockout channel from ^{6}He (240 MeV/u) impinging on a carbon target. The result obtained for ^{5}H is compared with microscopical calculations and analysed using the series expansion of the amplitudes of the three-body decay into hyperspherical harmonics. A broad structure in the t+n+n-relative energy spectrum with a width of 6 MeV (FWHM), peaked at 3 MeV, has been assigned to the ^{5}H resonance.

Key words: Nuclear Reactions. ^{12}C(^{6}He,n n t),^{12}C(^{6}He,n t), 240 MeV/u. Resonance States. ^{4}H, ^{5}H. Three-Body Correlations. Hyperspherical Harmonics.

PACS: 27.10.+h, 25.60.Gc

In the last decade, several experiments aimed to search for the ^{5}H resonance states (Refs. [1–7]) have given interesting but contradictory results.

The structure of an unbound heavy hydrogen system (A$\geq$4) is expected to be similar to that of neutron-rich helium isotopes, namely, an inert core surrounded by valence neutrons [8,9]. Thus, the ^{5}H isotope, with an even neutron number, could have a resonance at low energy due to the neutron pairing energy. An estimate based on the ^{4}H ground state energy recommended in the compilation [1] (E_R=3.2 MeV) and neutron pairing energy for ^{6}He (E_{pair}=2.75 MeV) used as an uppermost limit for E_{pair} in ^{4}H, results in conclusion that ^{5}H is unbound by at least by $E_R(^5H) = 2E_R(^4H) - E_{pair} = 3.6$ MeV.

Let us consider only the experiments made in the last ten years. The experiments can be subdivided into two groups.

On the one side, an evidence for ^{5}H as a broad state at 5.2(4) MeV was obtained in studies of ^{7}Li(^{6}Li,^{8}B) [2]. A recent experiment reports the ground state at 5(1) MeV with a width of 3 MeV in a π^- absorbtion by ^{9}Be [5]. Thus, these data are in agreement with the consideration made above.

On the other side, a resonance energy equal to 1.1 MeV is recommended in the recent review of A=5-7 [1]. This value is based on the measurement with

[1] on leave from RRC “Kurchatov Institute”, 123182 Moscow, Russia

a ^{1}H(^{6}He,pp t) reaction [3]. The observation of the ^{5}H ground state at 1.7(3) MeV with a width of 1.9(4) MeV in the same reaction was reported in ref. [4]. The latest news from CAEN [7] support of the result obtained in [4]. The ^{3}H(t,p n t) reaction revealed a peak in the ^{5}H spectrum at the same energy as in Ref. [4] but with a width less than 500 keV [6]. These experiments are in contradiction with the estimate for $E_R(^5H)$ made above.

This paper is devoted to the experimental investigation of ^{4}H and ^{5}H studied in the one-proton knockout channel of ^{6}He (240 MeV/u) impinging on a carbon target. The relative energy spectra for t+n and t+n+n systems are reconstructed from the data and analysed. A comparison with three-body calculations is used in the t+n+n case. The interpretation of the data is done in the framework of an analysis using a restricted set of hyperspherical harmonics (HH) to obtain the relative weights of the predominant partial waves, and further to assign the spin and parity to the structure seen in the energy spectrum. A detailed discussion is presented in ref. [10].

1 Experimental method and analysis procedure

The radioactive beam of 240 MeV/u ^{6}He was produced in an 8 g/cm^2 Be production target by fragmentation of a primary ^{18}O (340 MeV/u) beam from the heavy-ion synchrotron SIS at GSI, and subsequently separated in the fragment separator FRS by magnetic analysis. The beam was then directed towards a carbon target (thickness 1.87 g/cm^2) placed directly in front of a large-gap dipole magnetic spectrometer, ALADIN. In the present paper only events containing a charged triton fragment and neutrons were chosen for the analysis. The tritons produced in the ^{6}He fragmentation were deflected and analyzed in the dipole magnet ALADIN in conjunction with position-sensitive multi-wire drift chambers and a plastic time-of-flight wall. The neutrons, recorded in coincidence with the tritons, were detected in the large area neutron detector, LAND. The momentum vectors of the triton and the neutrons were determined for each separate reaction event.

The momentum distributions of the tritons and neutrons reveal a peak centered at about projectile velocity in the longitudinal direction with about the same widths for their longitudinal and transverse components in the projectile center-of-mass system. The measured probability to detect two neutrons in coincidence with the triton is about three times larger than in the α channel where the one-neutron knockout channel dominates the reaction mechanism.

These facts give evidence for a dominant contribution of the proton knockout channel, which leads to a final state of $t+n+n$, where all three fragments are close in momentum space.

2 Invariant mass spectra

The relative energy spectra in the few-body system, which are equivalent to the invariant mass spectra with the subtracted masses af the involved fragment, are a widely used tool while searching for particle resonances.

First, we look at the relative energy spectrum $d\sigma/dE_{tn}$ in the $t+n$ system. The measured large probability of having two neutrons with a small relative momentum, and thus, with strong interaction between them, leads to difficulties in the interpretation for the properties of the t+n system. The ^{4}H result presented in Fig. 1 (left panel) was obtained from events where only one neutron was detected in LAND in coincidence with the triton and thus well separated in momentum space from the second neutron.

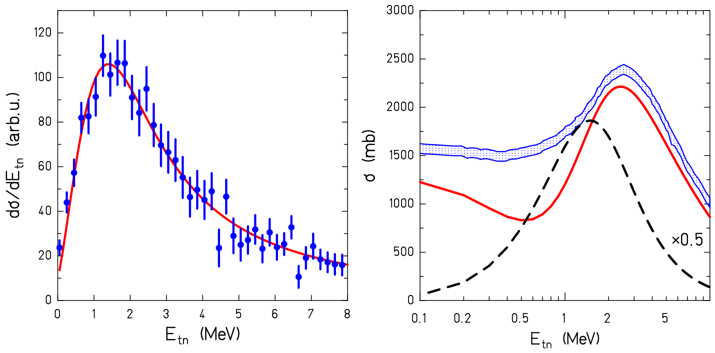

Fig. 1. Left panel: The ^{4}H energy spectrum. The solid line is the result of a fit using a Breit Wigner expression. Right panel: Measured n+^{3}H total cross section (shadowed zone) from ref. [13] compared with the R-matrix prediction (solid line) for an isolated resonance and p-wave potential scattering. The separate resonance contribution is shown by the dashed line. The resonance parameters were obtained in the present experiment.

The fit to the experimental energy distribution was done using a Breit-Wigner shaped resonance, as defined in [12], with inclusion of the experimental resolution and acceptance of the setup. The fit resulted in the following parameters: E_R=2.67(31) MeV and Γ^{obs}=3.28(23) MeV, where only a p-wave was considered and the channel radius R was fixed at 4 fm.

The extracted parameters are in agreement with experiments with nuclear reactions of different kinds looking for ^{4}H (see compilation [1]) and lower than the recommended value 3.19 MeV [1]. One may note that the maximum in the measured invariant mass spectrum is at about 1.6 MeV while the experimental excitation function of the n+^{3}H total cross section is peaked at about 2.6 MeV [13]. In order to understand this effect, the elastic scattering cross section was calculated using the R-matrix expression (formulae 1.14 on p. 322 in Ref. [12]). By using the resonance parameters obtained in the present work, and without any additional parameters the peak position in Ref. [13] could be reproduced. The result is shown in the right panel of Fig. 1. The interference between potential and resonance scattering is the reason for the shift of the maximum. Thus, for a broad state, the position of the maximum in the experimental distribution is depending on the reaction mechanism.

2.1 The ^5H case

We now turn to the ^{5}H case where two neutrons are registered in coincidence with the residual charged fragment.

We first introduce a set of normalized Jacobi momentum coordinates:

$$\begin{aligned} \mathbf{q}_{12} &= \left(\frac{\mu_{12}}{2}\right)^{\frac{1}{2}} \left(\frac{\mathbf{p}_1}{m_1} - \frac{\mathbf{p}_2}{m_2}\right); \\ \mathbf{q}_{3-12} &= \left(\frac{\mu_{3-12}}{2}\right)^{\frac{1}{2}} \left(\frac{\mathbf{p}_3}{m_3} - \frac{\mathbf{p}_1 + \mathbf{p}_2}{m_1 + m_2}\right) \end{aligned} \tag{1}$$

where m_i, μ_{12}, μ_{3-12}, $\mathbf{p}_i$, $i = 1, 2, 3$ are masses, reduced masses and momenta of the particles in the projectile rest frame. Two different Jacobi coordinate systems are used, **A** and **B**. In **A** indices 2,3 are related to neutrons and 1 to the triton, while in **B** 1 and 2 are related to the neutrons while 3 stands the triton. The total kinetic energy in the t+n+n system is then equal to $E_{tnn} = q_{12}^2 + q_{3-12}^2$.

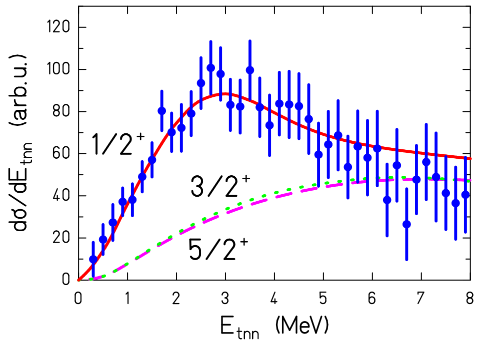

Fig. 2. The energy spectrum of the $t+n+n$-system. The solid line is the result of a three-body microscopic calculation, assuming $I^\pi = 1/2^+$ [8], the dotted and dashed lines correspond to the $3/2^+$ and $5/2^+$ state, respectively.

The distribution of the total kinetic energy in the three body system E_{tnn}, which is an equivalent of the invariant mass spectrum, is shown in Fig. 2. The observed structure exhibits a width of about 6 MeV FWHM with a maximum at about 3 MeV.

The spectrum was compared with calculations made within a strict three-body ($t + n + n$) dynamics and using a HH expansion [8]. As can be seen in Fig. 2, good agreement between the shape of the calculated ground state ($I^\pi = 1/2^+$) spectrum and the experimental data is achieved. However, to independently confirm the $I^\pi = 1/2^+$ assignment, an analysis of the energy and angular correlations in the t+n+n system was performed.

3 Energy and angular correlations in the $t+n+n$ system

3.1 Three body correlations

Neglecting the orientation of the whole system, the three-body configuration is uniquely described by the angle ϑ between the Jacobi momenta $\mathbf{q}_{12}$ and $\mathbf{q}_{3-12}$, by the total energy of the three-body system E_{tnn} and by the energy shared by a pair of particles $\varepsilon = q_{12}^2/E_{tnn}$. Finally, the energy and angular correlations in the $t+n+n$ system can be described by a probability distribution $\mathcal{W}(\varepsilon,\vartheta)$, presenting the probability to find the system in a configuration in vicinity of definite values ε and ϑ.

This distribution was determined from experimental data and its projections on the angular and energy axis in the two different Jacobi coordinates are shown in Fig. 3 where (1) and (2) are shown in Jacobi system $\mathbf{A}$ $(n-tn)$ and, (3) and (4) in system $\mathbf{B}$ $(t-nn)$.

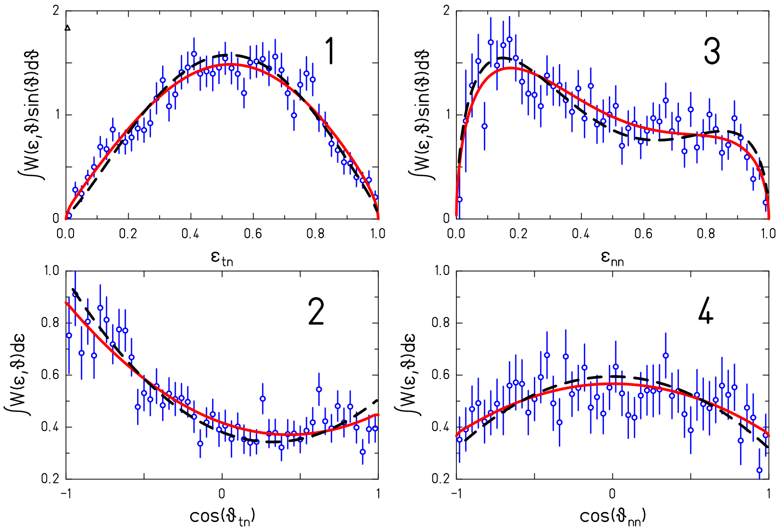

Fig. 3. Energy and angular correlations. Figures (1) and (2) are shown in Jacobi system $\mathbf{A}$ $(n-tn)$ and, (3) and (4) in system $\mathbf{B}$ $(t-nn)$. The solid lines represent the fit to the distributions via expansion on hyperspherical harmonics, the dashed lines corresponds to the same fit corrected for experimental resolution.

In order to determine the weights of the different partial waves in the $t+n+n$ system from experimental data, a method proposed in Ref. [14] was used. The method is based on a fitting procedure using the series expansion of the amplitudes of the three-body decay into HH. The HH are the eigenfunctions of the angular part of the Schrödinger equation in the six dimensional space. The proposed method represents a generalization of the Legendre polynomial expansion known from the two-body problem to the case of three-bodies.

Fitting the data, only components dominating the ^{6}He ground state were used: i.e. K = 0,2 and $l_{x(y)}$ = 0,1. Note, that these components exhaust 97%

of the norm of the ^{6}He ground-state wave function [11]. The expansion is characterized by a set of complex amplitudes $C_{SKl_xl_y}$ for the respective harmonics, where S is the total spin of the two neutrons, K the hypermomentum, and $l_{x(y)}$ are the angular momenta connected with $\mathbf{q}_{12}$ and $\mathbf{q}_{3-12}$ coordinates, respectively.

In system **B**, $(t-(nn))$, the antisymetrisation of the wave function with respect to the two neutrons results to $C_{0211}=0$. Moreover, the phase differences $\alpha_{SKl_xl_y}$ in system **A** are directly related to the phase difference β_{0200} in system **B**, namely $\alpha_{0211}=\alpha_{0200}+\pi=\beta_{0200}$.

Two independent fits were made. In the first fit, all seven parameters were kept free. The result for the corresponding system is shown in Table 1. Remarkably, $|C_{0211}|^2$ in system **B** was obtained equal to zero within statistical accuracy. Moreover, within an accuracy of a few degrees the relation between the phases mentioned above is fulfilled. These fitting procedures confirmed that the basic properties of the three-body system are well reproduced and demonstrate a high confidence level of the extracted parameters.

Table 1
Weights $|C_{SKl_xl_y}|^2$ of the different HH components in percent, and phases (α and β in degrees) obtained from fits. The errors given are statistical and all free parameters are shown in bold fonds.

Fit	$\mid C_{0000}\mid^2$	$\mid C_{0200}\mid^2$	$\mid C_{1211}\mid^2$	$\mid C_{0211}\mid^2$	β_{0200}	β_{0211}
B^1	17(4)	**46(3)**	**37(5)**	**0.02(9)**	**60(3)**	**0(180)**
B^2	18(3)	**45(2)**	**37(4)**	0.0	**61(2)**	-
Fit	$\mid C'_{0000}\mid^2$	$\mid C'_{0200}\mid^2$	$\mid C'_{1211}\mid^2$	$\mid C'_{0211}\mid^2$	α_{0200}	α_{0211}
A^1	17(4)	2.9(1)	37(4)	43(3)	**243(9)**	**61(3)**
A^2	18(3)	2.9(1)	37(4)	42(3)	241(2)	61(2)

The final fit was made using three free parameters, C_{0200}, C_{1211} and β_{0200}. All other parameters were fixed either by symmetry properties or transformation characteristics. The results are shown in rows B^2 and A^2 of Table 1, and a correspondence with experimental data is demonstrated by solid lines in Fig. 3. The dashed lines in Fig. 3 show the same distributions, corrected for experimental resolution.

In system **B** the configurations C_{0000} and C_{0200} straight forward result in $I^\pi=1/2^+$ of the $t+n+n$ system, some portion of the C_{1211} component can also be assigned to this spin and parity. From the weights given in Table 1, the conclusion is thus that the $I^\pi=1/2^+$ state in ^{5}H system is dominantly populated.

The resulting probability distribution $\mathcal{W}(\varepsilon,\vartheta)$ in Jacobi coordinate system **B** without distortions by the experimental resolution is shown in Fig. 4. The angular distributions are almost flat when the relative energy ε between the two neutrons is close either to 0 or to 1. However it behaves almost as $\sin^2\vartheta$

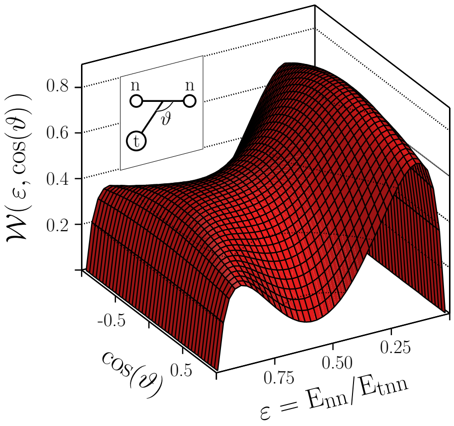

Fig. 4. Two dimensional plot of the probability distribution $\mathcal{W}(\varepsilon, \cos(\vartheta))$, extracted using a series expansion of the final state wave function into hyperspherical functions with amplitudes adjusted to fit the experimental data. The inset sketches the used coordinate system **B**.

when ε is close to 0.5. The latter is connected to the fact that the harmonic with $K = 2$, $S = 1$ mainly determines the correlations. Further, the energy distribution reveals two distinct peaks clearly seen in the vicinity of $\vartheta = 0$ and 180 degrees. The peaks are described mainly by the interference of harmonics with $K = 2$, $S = 0$ and $K = 0$, $S = 0$ and reflects the dynamical correlations which have been discussed for the ^{6}He wave function in microscopic calculations [11]. In the conjugated spatial coordinates the peaks correspond to di-neutron configuration with two neutrons forming a cluster on one side of the triton and to a cigar-like configuration where the neutrons are separated from each other by the triton core.

3.2 Comparison with nuclei close by

The structure of ^{5}H is expected to be an inert core surrounded by valence neutrons [8,9]. Thus, the ^{5}H isotope in its ground state should have similar structure as the ^{6}Be ground state while the excited states of ^{5}H should have resemblance to the ^{6}He first excited 2^+ state. The mentioned states in ^{6}Be and ^{6}He are well known examples for three-body decay and have been experimentally studied [14] by using the series expansion of the amplitudes into HH. Fig. 5 shows the comparison of energy and angular correlations for the three states ^{5}H, ^{6}Be(0^+), ^{6}He(2^+). Panel 3 demonstrates that in the shell-model equivalent Jacobi coordinate system **A**, the configuration with $l_x = l_y = 1$ dominates and the difference between ^{5}H, ^{6}Be(0^+) and ^{6}He(2^+) is small. However, the distributions for ^{6}Be(0^+) in panels 2 and 3 are much closer to the ^{5}H result as compared to ^{6}He(2^+). Thus, the conclusion can be drawn, that the correlations, observed in the present experiment resembles more ^{6}Be(0^+) and should correspond to ^{5}H in its ground $I^\pi = 1/2^+$ state.

Recently, $\mathcal{W}(\varepsilon, \vartheta)$ and the ^{5}H energy spectrum obtained in the present work

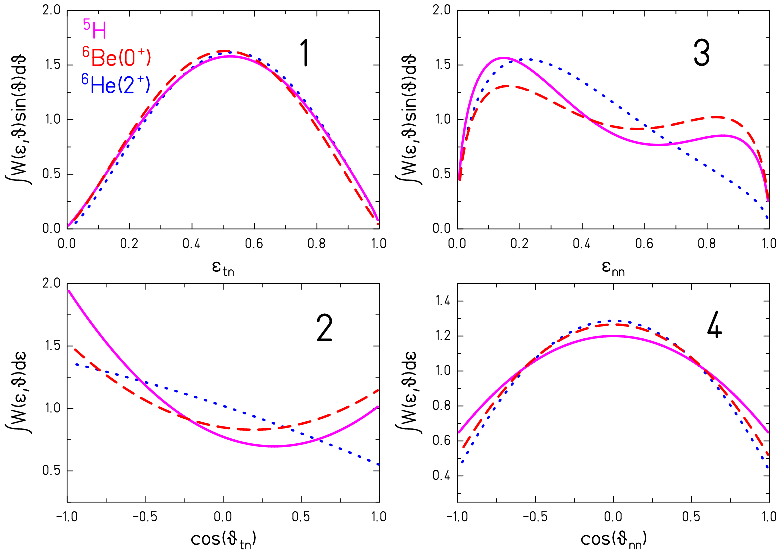

Fig. 5. Energy and angular correlations. Figures (1) and (2) are shown in Jacobi system **A** ($n-tn$) and, (3) and (4) in **B** ($t-nn$). The solid lines display the distributions obtained for ^{5}H, The dashed and dotted lines demonstrate the experimental results obtained for the three-body decay of ^{6}Be(0^+) and ^{6}He(2^+) states [14], respectively.

have been described by a model of a sudden one-proton knockout from ^{6}He [15] where the ^{6}He wave function was taken from microscopical three-body calculations.

By using the series expansion on a corresponding set of hyperspherical harmonics, the authors of ref. [15] also made a fit to $\mathcal{W}(\varepsilon,\vartheta)$ under the assumption that ^{5}H was obtained predominantly in its excited state. However, to reach the correspondence with the experimental data, the relative contribution of the excited state has been artificially increased several times in comparison with the prediction of the proton-knockout model and the calculated positions of the ^{5}H states have been as well artificially shifted towards lower energies. Thus the results of [15] support the conclusions made in the present paper.

4 Discussion and conclusion

The present result, taking into account the broadness of the structure, is in agreement with some earlier results [2,5]. The reaction channel selected in this experiment, however, can not reproduce the narrow structure seen in [4,6] and can not therefore shed light on their origin.

Incorrect interpretation of the data could, in principle, be a reason of the contradiction. In ref [4], the mechanism of the ^{1}H(^{6}He,p p t) reaction was assumed to be the ^{2}He emission. The argument for it was found in the relative energy distribution of two protons ($d\sigma/dE_{pp}$). The distribution was described by a Watson-Migdal model with the three-body phase space and under assumption of a zero-width resonance in ^{5}H. However, only about 10 MeV is avaliable for the sum of kinetic energies of all reaction products (t+2n+2p) and under such condition the ^{2}He channel cannot be isolated from other subsystems, as well as any other binary channel. The measured trend in $d\sigma/dE_{pp}$ can be reproduced when the five-body phase space is used, instead of the three-body phase space from ref. [4]. The result of the calculation is demonstrated in Fig. 6 (left panel) by the dashed line. The pp final state interaction taken into account with the phase shift determined by the effective-range approximation (a_{pp}=-7.8 fm) does not result to a better description of the data. However, a good representation can be achieved by inclusion of several types of different final state interaction: t+p, n+p etc.

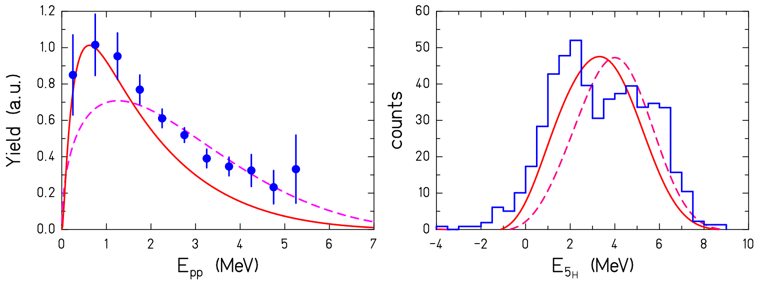

Fig. 6. Left panel: Relative energy distribution of two protons from the reaction $p(^6He, p\ p\ t)$. Right panel: Spectrum of ^{5}H from the reaction $p(^6He, p\ p\ t)$. The dashed lines display the result of a 5-body phase space calculation. The effect of additionally included final state interaction (FSI) leads to the solid lines (pp-FSI in left panel and nn-FSI in right panel. Experimental data are taken from ref. [4].

An enhancement at small energies can be seen in the ^{5}H experimental spectrum from ref. [4] in comparison with the five-body phase space calculations as shown by the dashed line in Fig. 6 (right panel). The nn-final state interaction taken into account results in a significantly better agreement with the experimental data as shown by the solid line. All the five particles are very close to each other in the phase space and the measured spectrum can thus be influenced by any of the particle unstable intermediate states (discrete states in ^{6}He, ^{5}He, ^{4}He above t+p+Xn threshold, singlet deuteron etc.) Thus, an explanation alternative to that given in ref. [4] is possible.

On the other hand, the narrow ^{5}H resonance may exist with other than t+n+n, e.g. a five-body compound structure where the triton core is dissolved by valence neutrons. In this case the resonance could be narrow as far as the only energetically possible decay channel t+n+n is structurally suppressed (See as an example, Ref. [16] where a $d+Xn$ structure of ^{4}H and ^{6}H is discussed). The proton knockout mechanism results mainly to the population of the ^{5}H states with a structure similar to that of ^{6}He, with an α-core replaced by a triton. The probability to populate any other ^{5}H configuration is low. The reactions at low energies are not so selective and population of the ^{5}H states with the different structure can be enhanced.

The conclusion based on the present analysis of the experimental data and on the comparison with the theoretical predictions [8,15] is that ^{5}H ground state with well pronounced $t + n + n$ cluster structure has existance as a broad state at the energy of about 3 MeV.

References

[1] D.R. Tilley, C.M. Cheves, J.L. Godwin, G.M. Hale, H.M. Hofmann, J.H. Kelley, C.G. Sheu, H.R. Weller, Nucl. Phys. **A708** (2002) 3, D.R. Tilley, H.R. Weller, G.M. Hale, Nucl. Phys. **A541** (1992) 1

[2] D.V. Aleksandrov, E.Yu. Nikolsky, B.G. Novatsky, D.N. Stepanov, *Proc. Intern. Conf. on Exotic Nuclei and Atomic Masses (ENAM-95), June 19-23, 1995, Arles, France* (1995) p. 329

[3] T.Kobayashi, K.Yoshida, A.Ozawa, I.Tanihata, A.Korsheninnikov, E.Nikolsky, T.Nakamura, Nucl. Phys. **A616** (1997) 223c

[4] A.A. Korsheninnikov, M.S. Golovkov, I. Tanihata, A.M. Rodin, A.S. Fomichev, S.I. Sidorchuk, S.V. Stepantsov, M.L. Chelnokov, V.A. Gorshkov, D.D. Bogdanov, R. Wolski, G.M. Ter-Akopian, Yu.Ts. Oganessian, W. Mittig, P. Roussel-Chomaz, H. Savajols, E.A. Kuzmin, E.Yu. Nikolsky, A.A. Ogloblin, Phys. Rev. Lett. **87** (2001) 092501

[5] M.G. Gornov, Ju.B. Gurov, S.V. Lapushkin, P.V. Morohov, M.S. Padorin, N.O. Poroshin, V.A. Pechurov, B.G. Sandukovskii, M.V. Tel'kushev, B.A. Chernyshev, *LII meeting on Nuclear Spectroscopy and Nuclear Structure, June 18-22, 2002, Moscow, Russia* Book of Abstracts (2002) p.70

[6] G.M. Ter-Akopian, *VII International School Seminar, May 27 - June 1, 2002, Dubna, Russia* Book of Abstracts (2002) p.87

[7] N.A. Orr, F.A. Marqués, Invited contribution to a Topical Issue of C.R.Acad.Sci. PARIS (2003), preprint LPCC 03-03, CAEN

[8] N.B. Shulgina, B.V. Danilin, L.V. Grigorenko, M.V. Zhukov, J.M. Bang, Phys. Rev. **C62** (2000) 014312

[9] P. Descouvemont, A. Kharbach, Phys. Rev. **C63** (2001) 027001

[10] M. Meister, L.V. Chulkov, H. Simon, T. Aumann, M.J.G. Borge, Th.W. Elze, H. Emling, H. Geissel, M. Hellström, B. Jonson, J.V. Kratz, R. Kulessa, Y. Leifels, K. Markenroth, G. Münzenberg, F. Nickel, T. Nilsson, G. Nyman, V. Pribora, A. Richter, K. Riisager, C. Scheidenberger, G. Schrieder, O. Tengblad, Nucl. Phys. **A723** (2003) 13

[11] B.V. Danilin, I.J. Thompson, J.S. Vaagen, M.V. Zhukov, Nucl. Phys. **A632** (1998) 383

[12] A.M. Lane, R.G. Thomas, Rev. Mod. Phys. **30** (1958) 257

[13] T.W. Phillips, B.L. Berman, Phys. Rev. **C22** (1980) 384

[14] O.V. Bochkarev, L.V. Chulkov, A.A. Korsheninnikov, E.A. Kuzmin, I.G. Mukha, G.B. Yankov, Nucl. Phys. **A505** (1989) 215, O.V. Bochkarev, A.A. Korsheninnikov, E.A. Kuzmin, I.G. Mukha, L.V. Chulkov, G.B. Yankov, Yad. Fiz. **575** (1994) 5; Phys. Atomic Nuclei **57** (1994) 1281

[15] L.V. Grigorenko, N.K. Timofeyuk, M.V. Zhukov, submitted to EPJ A 2003, L.V. Grigorenko, submitted to EPJ A 2003,

[16] J.M. Bang, F.A. Gareev, G.S. Kazacha, A.M. Kalinin, Phys. Scr. **41** (1990) 202